



## Origin of dolomite-ankerite cement in the Bravaisberget Formation (Middle Triassic) in Spitsbergen, Svalbard

Krzysztof P. KRAJEWSKI and Ewa WOŹNY

*Instytut Nauk Geologicznych PAN, Twarda 51/55, 00-818 Warszawa, Poland*  
*<kpkraj@twarda.pan.pl> <ew\_ja@wp.pl>*

**Abstract:** The organic carbon (OC)-rich, black shale succession of the Middle Triassic Bravaisberget Formation in Spitsbergen contains scattered dolomite-ankerite cement in coarser-grained beds and intervals. This cement shows growth-related compositional trend from non-ferroan dolomite (0–5 mol %  $\text{FeCO}_3$ ) through ferroan dolomite (5–10 mol %  $\text{FeCO}_3$ ) to ankerite (10–20 mol %  $\text{FeCO}_3$ , up to 1.7 mol %  $\text{MnCO}_3$ ) that is manifested by zoned nature of composite carbonate crystals. The  $\delta^{13}\text{C}$  (-7.3‰ to -1.8‰ VPDB) and  $\delta^{18}\text{O}$  (-9.4‰ to -6.0‰ VPDB) values are typical for burial cements originated from mixed inorganic and organic carbonate sources. The dolomite-ankerite cement formed over a range of diagenetic and burial environments, from early post-sulphidic to early catagenic. It reflects evolution of intraformational, compaction-derived marine fluids that was affected by dissolution of biogenic carbonate, clay mineral and iron oxide transformations, and thermal decomposition of organic carbon (decarboxylation of organic acids, kerogen breakdown). These processes operated during Late Triassic and post-Triassic burial history over a temperature range from approx. 40°C to more than 100°C, and contributed to the final stage of cementation of the primary pore space of siltstone and sandstone beds and intervals in the OC-rich succession.

**Key words:** Arctic, Svalbard, Middle Triassic, cementation, petrography, geochemistry, carbon and oxygen isotopes.

### Introduction

Organic carbon (OC)-rich intervals of the Mesozoic sedimentary succession in Svalbard (Harland 1997; Mørk *et al.* 1999) contain common carbonate deposits (calcite, dolomite, ankerite, and siderite) originated over a range of subsurface diagenetic and burial environments. These deposits occur as isolated rock bodies in OC-rich shales and mudstones (beds, lenses and concretions) as well as in the form of pore-filling to replacive cement in siltstone and sandstone interbeds. The petrographic and isotopic data collected so far suggest that at least part of these deposits originated as a result of stages of microbiological and thermal degradation



Fig. 1. Sketch map of the Svalbard archipelago showing location of stratotype section of the Bravaisberget Fm at Bravaisberget, western Nathorst Land (NL). B – Bellsund; VM – Van Mijenfjorden; VK – Van Keulenfjorden.

of organic carbon, thus affecting both the petroleum potential of the succession as well as the reservoir properties of coarser-grained intervals (Krajewski 2000a–e, 2002, 2004, 2008; Krajewski *et al.* 2001, 2007; Krajewski and Luks 2003).

This paper elucidates origin of dolomite-ankerite cement in the Middle Triassic Bravaisberget Fm in Spitsbergen on the basis of petrographic and geochemical analysis of its stratotype section at Bravaisberget in western Nathorst Land (Fig. 1). This section was a subject of geological, geochemical and isotopic investigations (Krajewski *et al.* 2007; Karcz 2008). The results show that the Bravaisberget Fm there occurs just beneath the oil window maturity level, and contains common carbonate cements throughout the succession. It is therefore suitable for conducting a study on carbonate diagenesis related to stages of degradation and maturation of organic carbon and hydrocarbon generation in the succession. From a detailed examination of cement paragenesis, its elemental and isotopic composition, and relative timing in the diagenetic sequence of events, we make an attempt to characterize the pore fluids and metal and carbon sources involved during the dolomite-ankerite cementation.

## Geological background

The Middle Triassic Bravaisberget Fm in western Spitsbergen embraces an OC-rich succession of black shales with (phosphatic) siltstone and sandstone intercalations (Passhatten Mb), which is overlain by phosphatic, calcite-cemented sandstones (Somovbreen Mb) and siliceous sandstones (Van Keulenfjorden Mb) (Fig. 2). It records a second-order transgressive-regressive cycle in the Svalbard basin that was widely influenced by high biological productivity conditions leading to increased content of organic carbon in sediments and phosphogenesis (Mørk *et al.* 1982, 1989; Krajewski 2000a, b). The association of organic carbon (mostly kerogen Type II) and authigenic phosphate (nodular, crust-like, and peloidal accumulations) is striking throughout the succession (Krajewski 2000d, e). In western Nathorst Land, the formation (> 200 m thick) occurs at eastern margin of the West Spitsbergen Thrust-and-Fold Belt, being involved in a wide monoclinal structure that dips eastwards (Krajewski *et al.* 2007). Burial under the overlying Jurassic and Cretaceous deposits as well as the Cenozoic orogenesis have led to maturation of organic carbon and expulsion of most of the hydrocarbons from the formation. Rock-Eval characteristics suggest that residual carbon dominates its organic pool (Karcz 2008). Carbonate cements occur throughout the succession, being represented by the calcite and dolomite-ankerite varieties (Krajewski *et al.* 2007). Petrographic analysis suggests that the calcite cement widely pre-dates formation of the dolomite-ankerite one (Krajewski 2000c). The calcite cement shows non-ferroan composition. It post-dates authigenic pyrite, and has carbon isotopic composition pointing to at least a partial source of carbonate from oxidative decomposition of organic carbon. This cement is interpreted to have developed in deeper parts of anoxic sulphidic diagenetic environment (Krajewski 2000c). However, very light isotopic composition of oxygen and striking recrystallization features indicate its thorough recrystallization and neoformation under burial. The calcite cement in the Bravaisberget Fm is restricted to the part of the succession deposited under normal marine conditions, *i.e.* to the Passhatten and Somovbreen members. The dolomite-ankerite cement is noted throughout the formation, though it becomes more common upwards the succession, attaining maximum concentration in the topmost Van Keulenfjorden Mb. It usually occurs in the form of minute crystals scattered in the matrix. It was suggested that this cement developed at later stages of diagenesis under increased burial, though detailed relations remain unknown (Krajewski *et al.* 2007; Krajewski 2008).

## Materials and methods

Sixteen samples of sandstones and siltstones from the Bravaisberget Fm at Bravaisberget were analyzed in detail: 9, 3, and 4 from the Passhatten, Somovbreen,

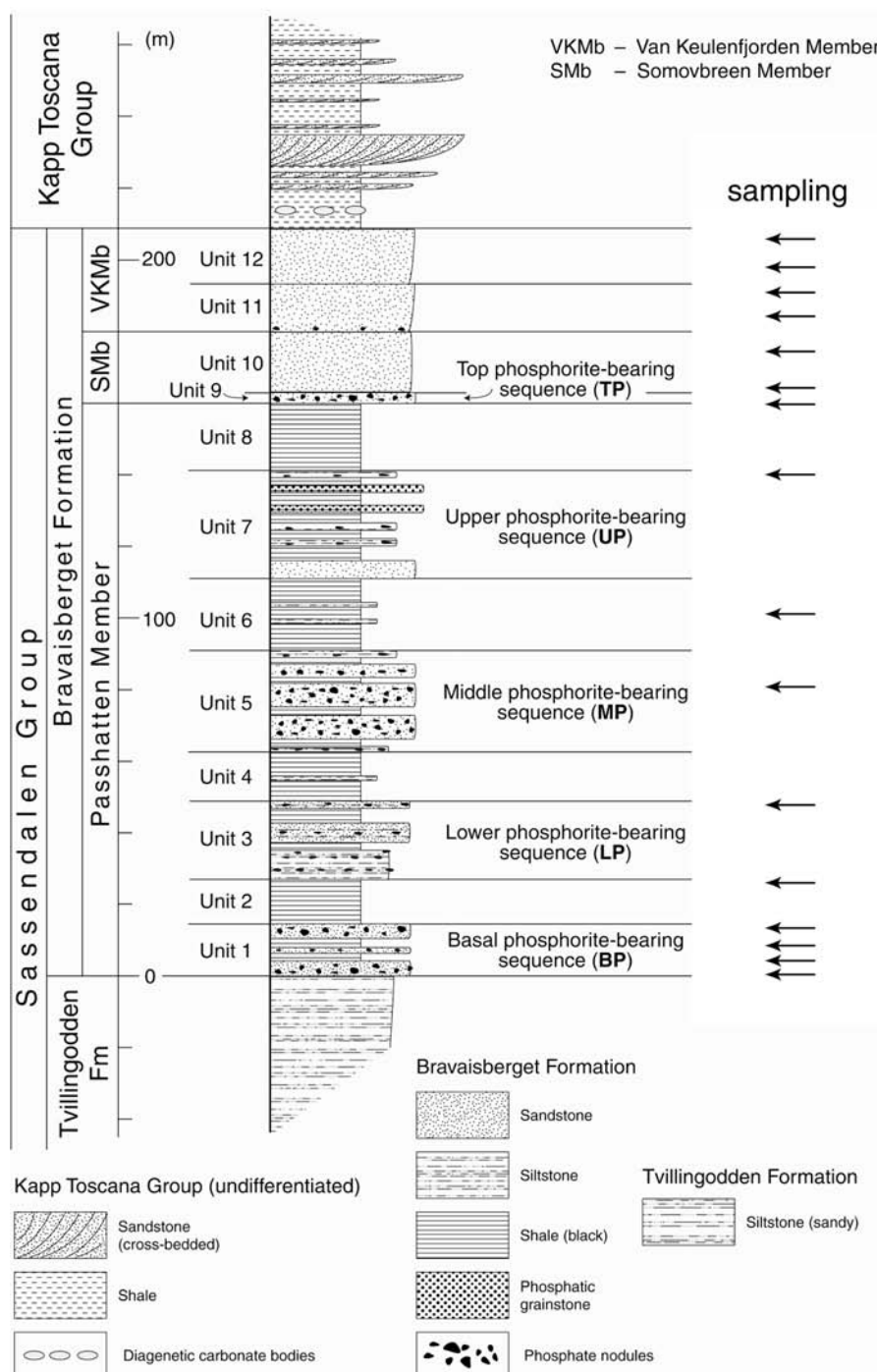


Fig. 2. Stratotype section of the Bravaisberget Fm at Bravaisberget showing its lithostratigraphic subdivision and position of samples analyzed in this paper. After Krajewski *et al.* (2007).

and Van Keulenfjorden members, respectively. Location of the samples is shown in Figure 2. All the samples were analyzed using conventional petrographic methods, including transmitted (TLM) and reflected (RLM) light microscopy, cathodoluminescent light microscopy (CL), back-scattered electron imaging (BSE), and energy-dispersive X-ray spectroscopy (EDS). BSE images were obtained using a JEOL JSM-840A microscope operating at 15 kV acceleration voltage. Quantitative EDS analyses of dolomite-ankerite cement were obtained on the same microscope equipped with a THERMO NORAN VANTAGE EDS system. Operating conditions were 15kV acceleration voltage, 1 to 5  $\mu\text{m}$  beam diameter, and 100-s counting time. Detection limits of the analyzed elements (Ca, Mg, Fe, Mn) were better than 0.1 wt. %. EDS data were recalculated as cation mol fractions to facilitate comparisons among samples.

Mineral composition of the samples was analyzed by means of X-ray diffraction (XRD). Samples were ground to < 63  $\mu\text{m}$  fraction. Diffraction patterns were recorded on a SIGMA 2070 diffractometer using a curved position sensitive detector in the range 2–120° 2 $\theta$  with CoKa radiation and 20 hour analysis time. DIFFRACTIONEL software v. 03/93 was used to process the obtained data.

Eight samples were analyzed for the carbon and oxygen isotopic composition of carbonate. Crushed samples were hand picked under a binocular microscope to provide material with maximum content of carbonate cement. Carbonate CO<sub>2</sub> was produced from samples by reaction with anhydrous phosphoric acid ( $d = 1.90 \text{ g cm}^{-3}$ ) under vacuum. In an attempt to discriminate between the calcite and dolomite-ankerite, the samples were treated by a progressive acid extraction. CO<sub>2</sub> from samples was collected after 15 to 30 minutes of reaction at 25°C, and after 48 hours at 50°C, with portion of gas discarded after 4 hours and 24 hours at 25°C. CO<sub>2</sub> collected in these steps represents calcite and dolomite-ankerite. The procedure was verified by XRD. Isotopic  $^{13}\text{C}/^{12}\text{C}$  and  $^{18}\text{O}/^{16}\text{O}$  ratios were determined using a FINNIGAN MAT DELTA PLUS spectrometer working in dual inlet mode with universal triple collector. The results are expressed as  $\delta^{13}\text{C}$  and  $\delta^{18}\text{O}$  notations with respect to VPDB standard (Vienna PeeDee Belemnite). Analytical reproducibility in laboratory was better than  $\pm 0.05\text{\textperthousand}$  and  $\pm 0.1\text{\textperthousand}$  for  $\delta^{13}\text{C}$  and  $\delta^{18}\text{O}$ , respectively. The results of calcite cement are addressed elsewhere (E. Woźny, in preparation), and not included in this paper.

The paleotemperatures of precipitation of the dolomite-ankerite cement were estimated on the basis of  $\delta^{18}\text{O}$  values using the following oxygen isotope mineral-water fractionation equations:  $1000 \ln \alpha (\text{dolomite-water}) = 2.78 \times 10^6 T^2 + 0.91$  (Land 1985); and  $1000 \ln \alpha (\text{ankerite-water}) = 2.78 \times 10^6 T^2 + 0.11$  (Fisher and Land 1986).

## Results

**Petrography.** — The dolomite-ankerite cement occurs in the form of minute rhombs (20–100  $\mu\text{m}$ ) scattered in the primary pore space of siltstone to sandstone

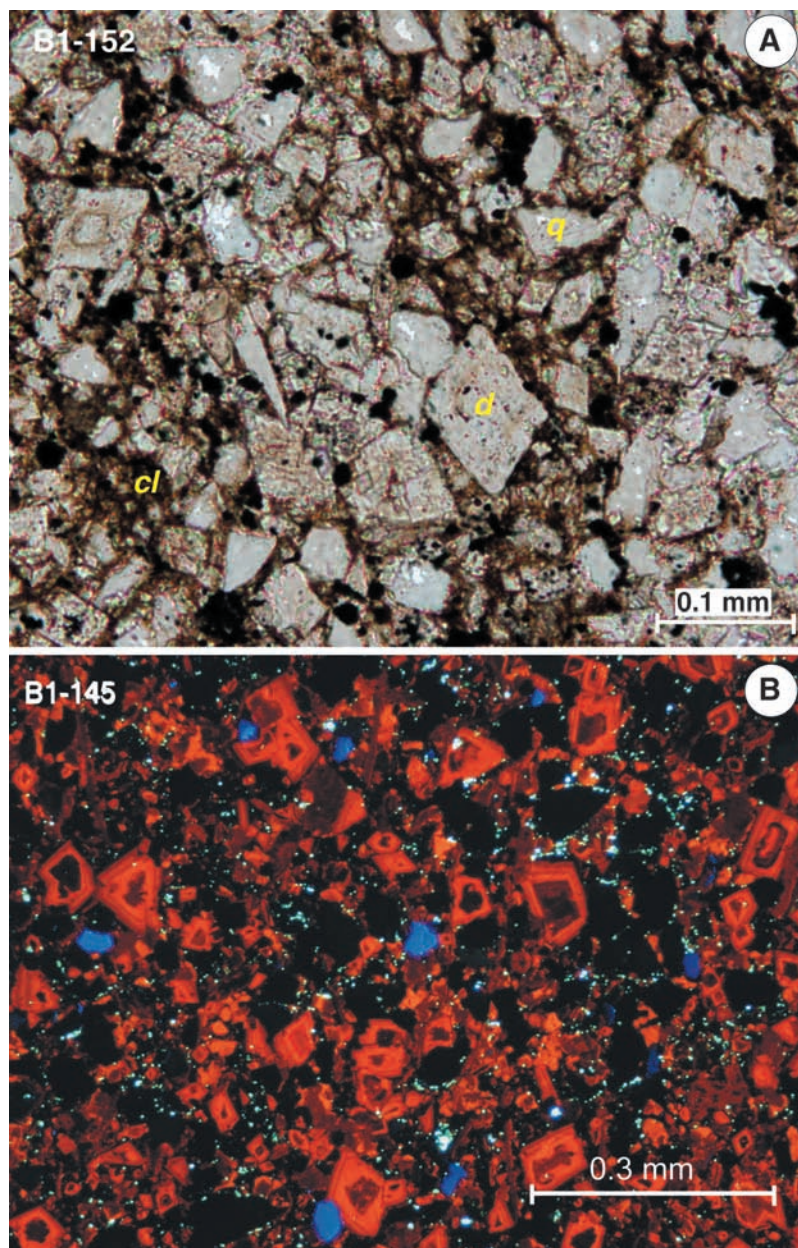


Fig 3. **A.** TLM photomicrograph of muddy sandstone of the Somovbreen Mb showing dolomite-ankerite rhombs (d) in primary pore space of sediment dominated by quartz grains (q) and clay minerals (cl). **B.** CL image of dolomite-ankerite rhombs in the Passhatten Mb showing their zoned internal structure.

beds and intervals (Fig. 3). Rare dolomite-ankerite crystals are also observed in black shale intervals, where they show emplacive growth associated with compac-

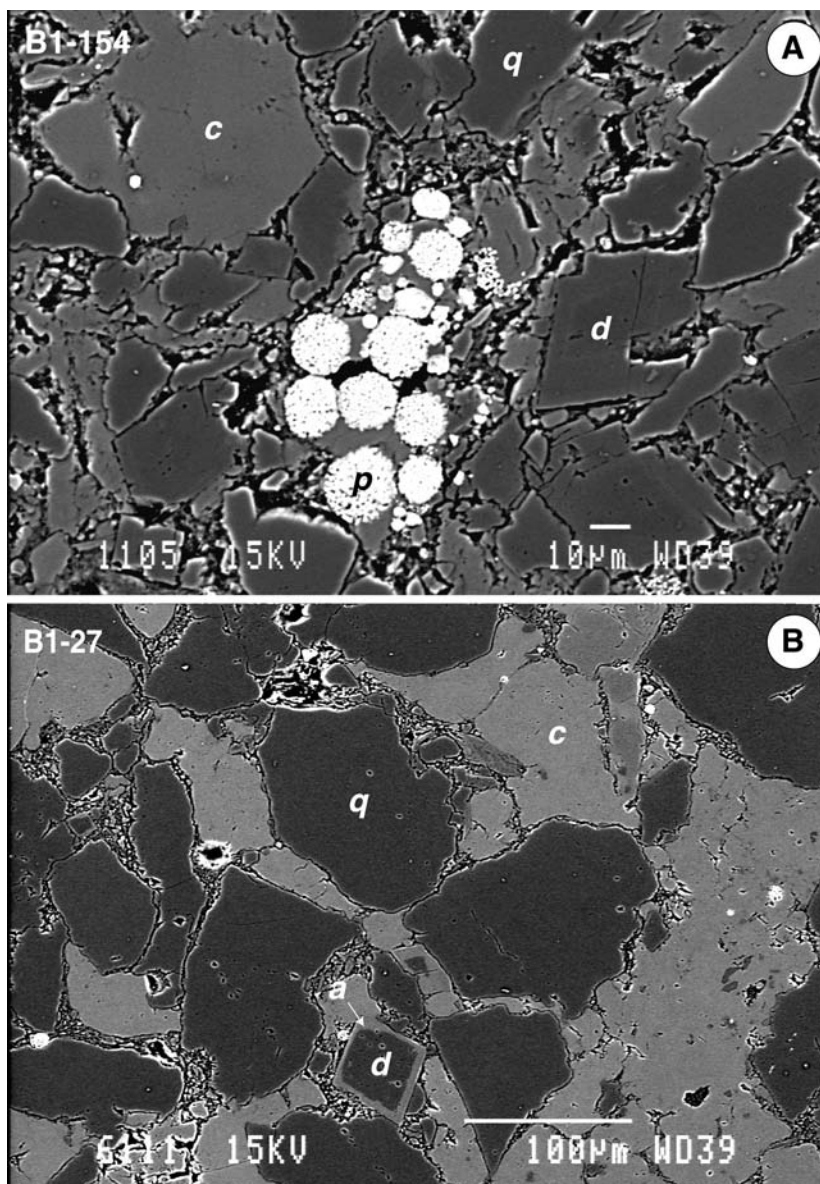


Fig. 4. **A.** BEI image of paragenetic sequence of cements in quartz (q) siltstone of the Somovbreen Mb showing authigenic pyrite frambooids (p), calcite (c), and dolomite-ankerite (d). **B.** BEI image of quartz (q) sandstone of the Passhatten Mb showing void-filling blocky calcite (c) and dolomite (d) to ankerite (a) zoned crystal. For bed numbering see Krajewski *et al.* (2007).

tion of the sediment. Dolomite-ankerite post-dates both the authigenic pyrite and void-filling calcite, though the latter shows ubiquitous recrystallization to form interlocking, blocky mosaic (Fig. 4). Most of the rhombs exhibit zonation in CL and BSE images. They have non-luminescent, massive cores coated by outer zones

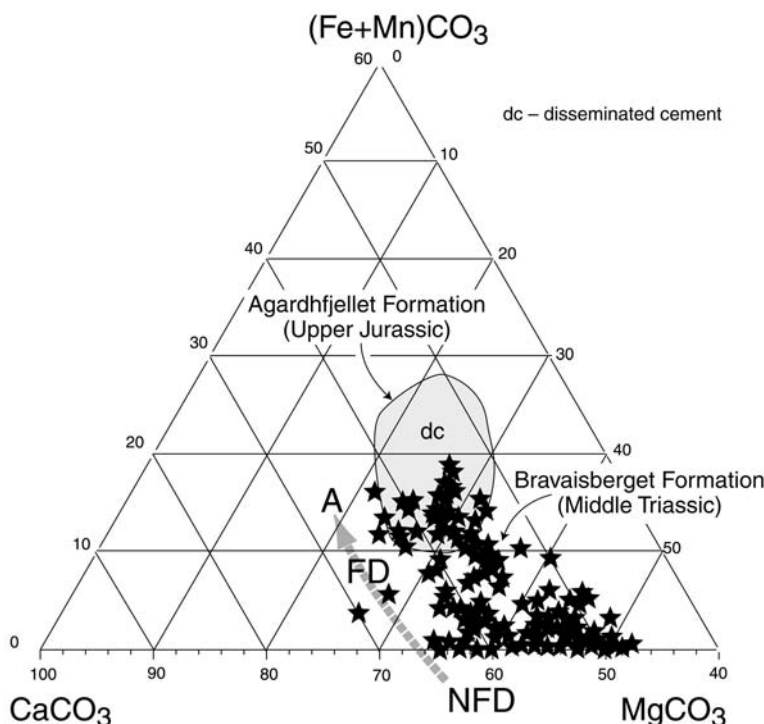


Fig. 5. Ternary diagram illustrating chemical composition of dolomite-ankerite cement in the Bravaisberget Fm. NFD – non-ferroan dolomite; FD – ferroan dolomite; A – ankerite. Field of ankerite cement in the Agardhfjellet Fm (Upper Jurassic) after Krajewski *et al.* (2001).

showing orange to red CL colours and brighter colour under BSE. In external zones of some of the crystals, there occur minute bitumen inclusions (1–4 µm), which are also noted in rudimentary voids of the siltstones and sandstones as well as in clay-rich matrices of black shales.

**Major element geochemistry.** — The results of EDS compositional analyses of dolomite-ankerite cement are shown in Fig. 5. There are three chemical varieties of the cement arranged in a growth-related compositional trend, from non-ferroan dolomite (NFD) through ferroan dolomite (FD) to ankerite (A). Detailed analyses of individual crystals show that massive cores are composed mostly of NFD, which in several cases grades outward to FD (Figs 6–8). The outer zone that usually coats the cores with sharp boundary is composed of A or FD with high content of iron. NFD is volumetrically the most abundant cement, though there are cementation horizons showing nearly equal amounts of dolomite and ankerite, in the Van Keulenfjorden Mb in particular. The increase of the content of iron (up to 20 mol %  $\text{FeCO}_3$ ) in composite crystals is positively correlated with similar increase of the content of manganese (up to 1.7 mol %  $\text{MnCO}_3$ ), and is associated with CL activation. There is no significant difference in mean chemical composi-

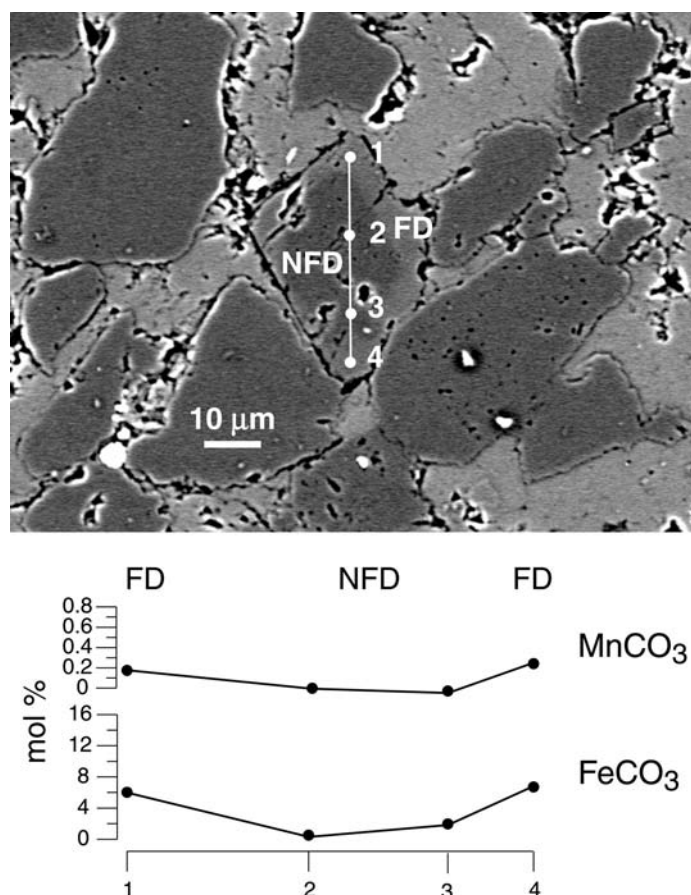


Fig. 6. Compositional changes in dolomite-ankerite cement (I). Non-ferroan dolomite (NFD) to ferroan dolomite (FD) growth trend.

tion of the crystal cores and outer zones in the Passhatten, Somovbreen and Van Keulenfjorden members. The compositions, calculated from more than 800 point EDS analyses, are: core –  $(\text{Ca}_{1.16}\text{Mg}_{0.81}\text{Fe}_{0.025}\text{Mn}_{0.005})(\text{CO}_3)_2$ , outer zone –  $(\text{Ca}_{1.19}\text{Mg}_{0.60}\text{Fe}_{0.20}\text{Mn}_{0.01})(\text{CO}_3)_2$ ; core –  $(\text{Ca}_{1.17}\text{Mg}_{0.81}\text{Fe}_{0.016}\text{Mn}_{0.004})(\text{CO}_3)_2$ , outer zone –  $(\text{Ca}_{1.20}\text{Mg}_{0.64}\text{Fe}_{0.15}\text{Mn}_{0.01})(\text{CO}_3)_2$ ; core –  $(\text{Ca}_{1.17}\text{Mg}_{0.82}\text{Fe}_{0.009}\text{Mn}_{0.001})(\text{CO}_3)_2$ , outer zone –  $(\text{Ca}_{1.130}\text{Mg}_{0.64}\text{Fe}_{0.25}\text{Mn}_{0.01})(\text{CO}_3)_2$ , respectively.

**Carbon and oxygen isotopes.** — The obtained  $\delta^{13}\text{C}$  and  $\delta^{18}\text{O}$  values of dolomite-ankerite cement are cross-plotted in Fig. 9. The  $\delta^{13}\text{C}$  and  $\delta^{18}\text{O}$  values fall in the ranges between  $-7.3\text{\textperthousand}$  and  $-1.8\text{\textperthousand}$ , and between  $-9.4\text{\textperthousand}$  and  $-6.0\text{\textperthousand}$  VPDB, respectively. The results express isotopic composition of bulk rock dolomite-ankerite cement, which encompasses a sequence of compositional varieties. Consequently, the obtained values represent averages of isotopic compositions of NFD, FD, and A.

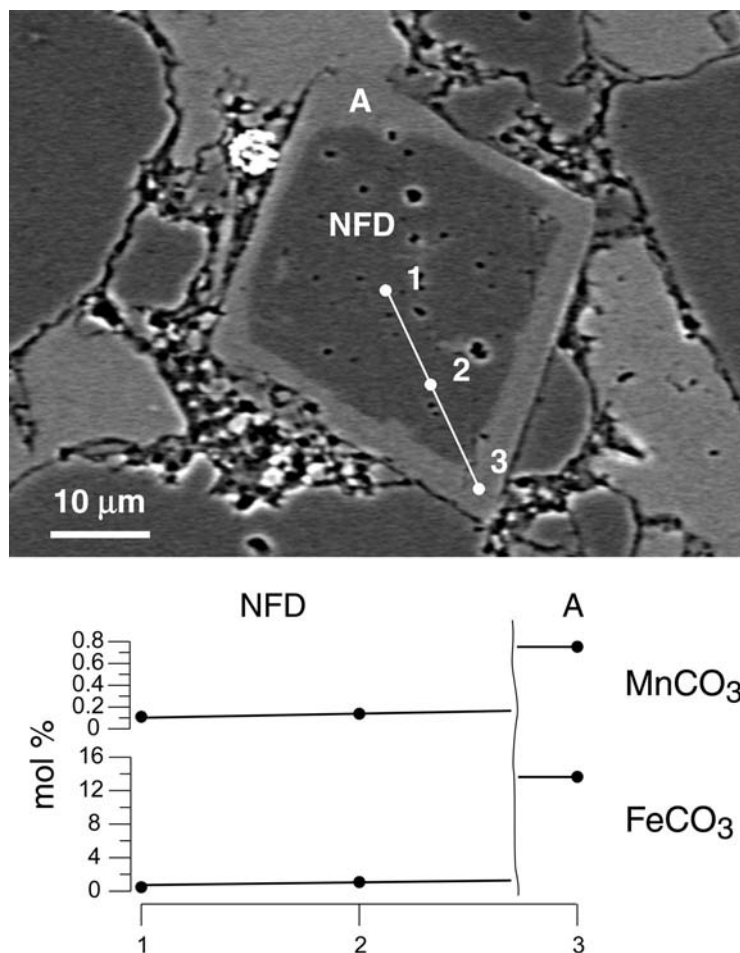


Fig. 7. Compositional changes in dolomite-ankerite cement (II). Non-ferroan dolomite (NFD) to ankerite (A) growth trend.

## Discussion

The dolomite-ankerite cement tends to occur in coarser-grained interbeds and thicker intervals in OC-rich shale succession of the Bravaisberget Fm. The available data suggest that the cement originated over a prolonged period of time in the diagenetic to burial environment.

**Timing of dolomite-ankerite precipitation.** — Determination of the relative timing of dolomite-ankerite cement precipitation is important in the interpretation of its diagenetic origin. Possible lines of evidence embrace reconstruction of the precipitation sequence from the cement paragenesis, its chemical composition, as well as from the carbon and oxygen isotopic record.

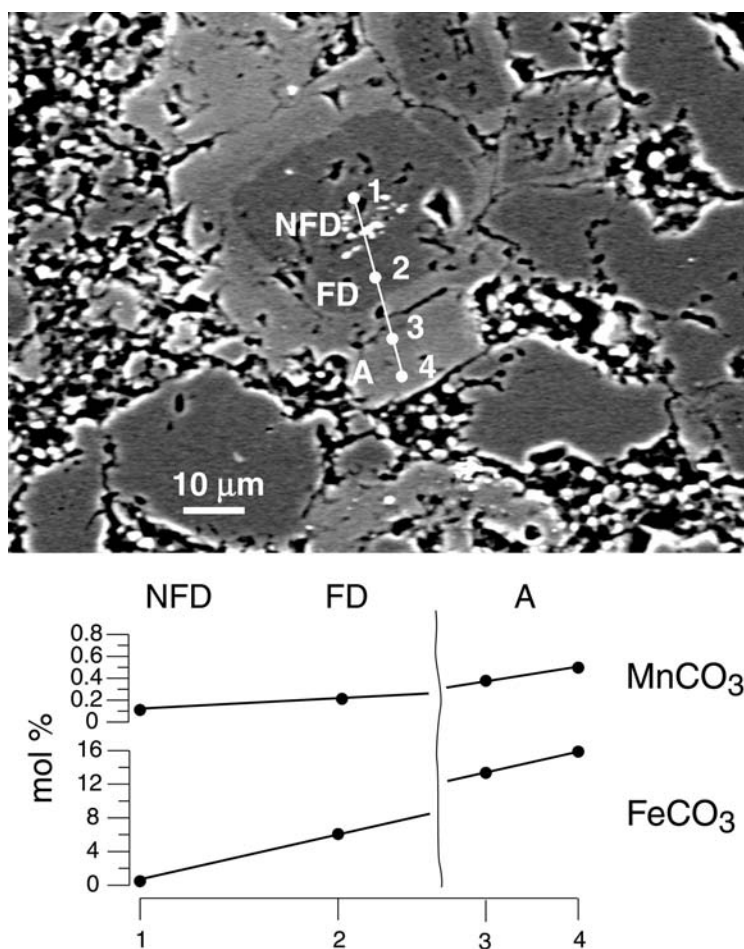


Fig. 8. Compositional changes in dolomite-ankerite cement (III). Non-ferroan dolomite (NFD) through ferroan dolomite (FD) to ankerite (A) growth trend.

**Constraints from cement paragenesis.** — Petrographic examination of cement paragenesis in the Bravaisberget Fm reveals that the dolomite-ankerite precipitated after formation of authigenic pyrite and non-ferroan calcite, which owed their origin to diagenetic processes in the sulphate reduction zone. Depending on sedimentation ratio and type of deposited organic matter, the thickness of this zone in OC-rich marine sediments may attain several hundreds of metres (Curtis 1987). Relations between the cement in siltstone to sandstone beds and in black shale intervals document displacive growth of at least a part of dolomite-ankerite crystals in muddy matrices. The youngest overgrowths in these crystals contain at places inclusions of syngenetic bitumen. Based on this evidence we can infer that the cement originated during and after significant compaction of the OC-rich, fine-grained sediments of the Triassic succession. Its

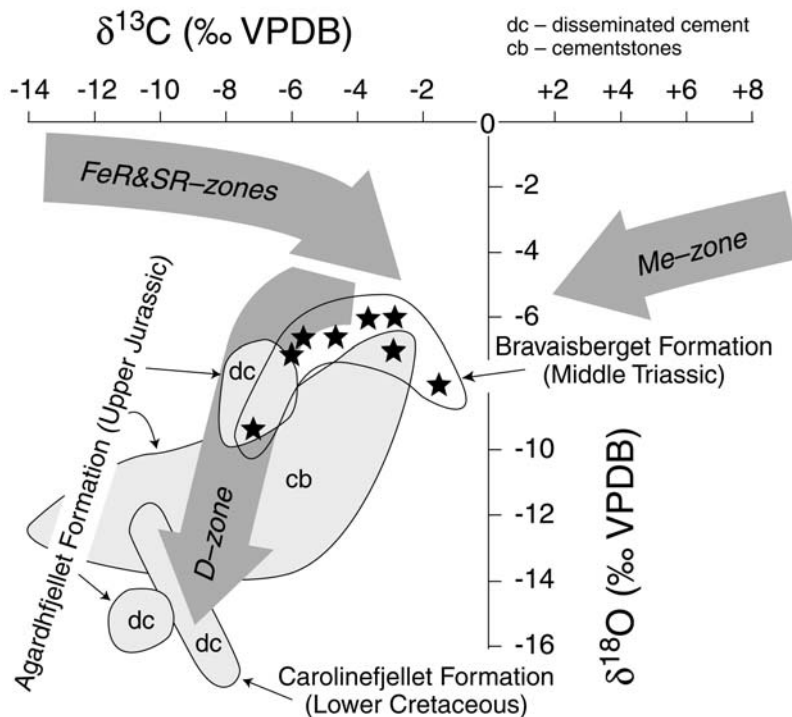


Fig. 9. Plot of  $\delta^{13}\text{C}$  (‰ VPDB) versus  $\delta^{18}\text{O}$  (‰ VPDB) of dolomite-ankerite cement in the Bravaisberget Fm. Diagenetic trends of carbonates formed in the iron reduction – sulphate reduction zones (FeR&SR zones), methanogenic zone (Me-zone), and thermal decarboxylation zone (D-zone) after Scotchman (1989). Fields of ankerite cement in the Agardhfjellet Fm (Uppere Jurassic) and in the Carolinefjellet Fm (Lower Cretaceous) after Krajewski *et al.* (2001), Krajewski (2002, 2004), and Krajewski and Luks (2003).

formation covered a spectrum of diagenetic environments, from early post-sulphidic ones to the onset of catagenic environment with kerogen breakdown and hydrocarbon generation.

**Constraints from elemental composition.** — The zoned nature and chemical composition of the dolomite-ankerite crystals suggest their formation from fluids characterized by changing content of calcium, magnesium, iron, and manganese cations. The common compositional trend from NFD through FD to A documents that the fluids evolved from calcium- and magnesium-dominated to the ones with elevated content of iron and manganese. The source of calcium was likely the original marine water as well as dissolution of biogenic carbonate, towards which there is ample petrographic evidence (Krajewski *et al.* 2007). The increasing content of  $\text{Fe}^{2+}$  and  $\text{Mn}^{2+}$  during burial can be correlated to transformations of clay minerals (illitization of chlorite) and dissolution of iron (hydr)oxides during progressive compaction of the shale succession. Similar transformations have been inferred for

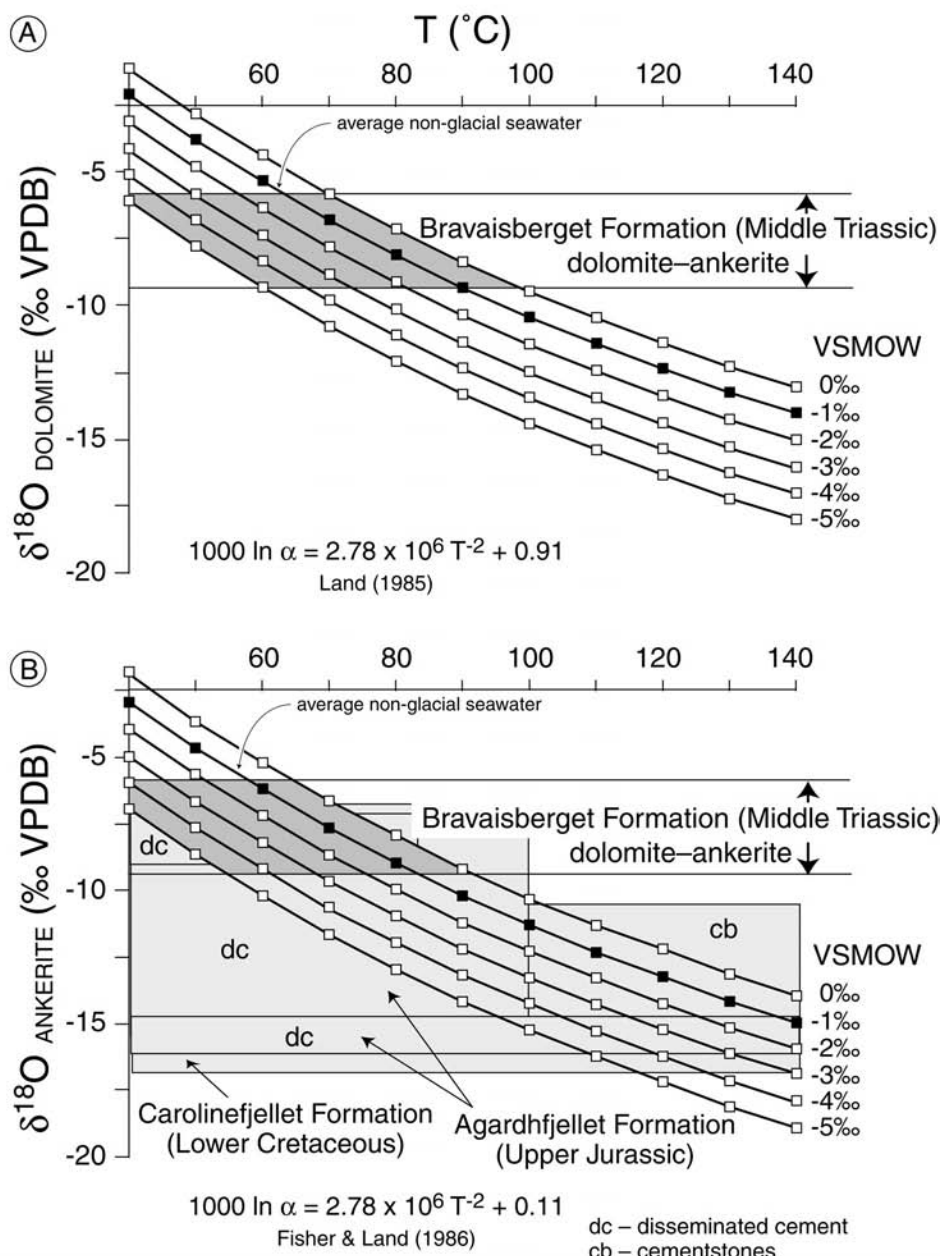


Fig. 10. Range of  $\delta^{18}\text{O}$  values (‰ VPDB) of dolomite-ankerite cement against precipitation temperature  $T$  (°C) of inorganic dolomite (A) and ankerite (B), with the calculated isotopic composition of diagenetic fluids from which they may have formed, assuming isotopic equilibrium. The water lines were calculated using the fractionation equation of Land (1985) for dolomite, and the equation of Fisher and Land (1986) for ankerite. Value ranges of ankerite cement in the Agardhfjellet Fm (Upper Jurassic) and in the Carolinefjellet Fm (Lower Cretaceous) after Krajewski *et al.* (2001), Krajewski (2002, 2004), and Krajewski and Luks (2003).

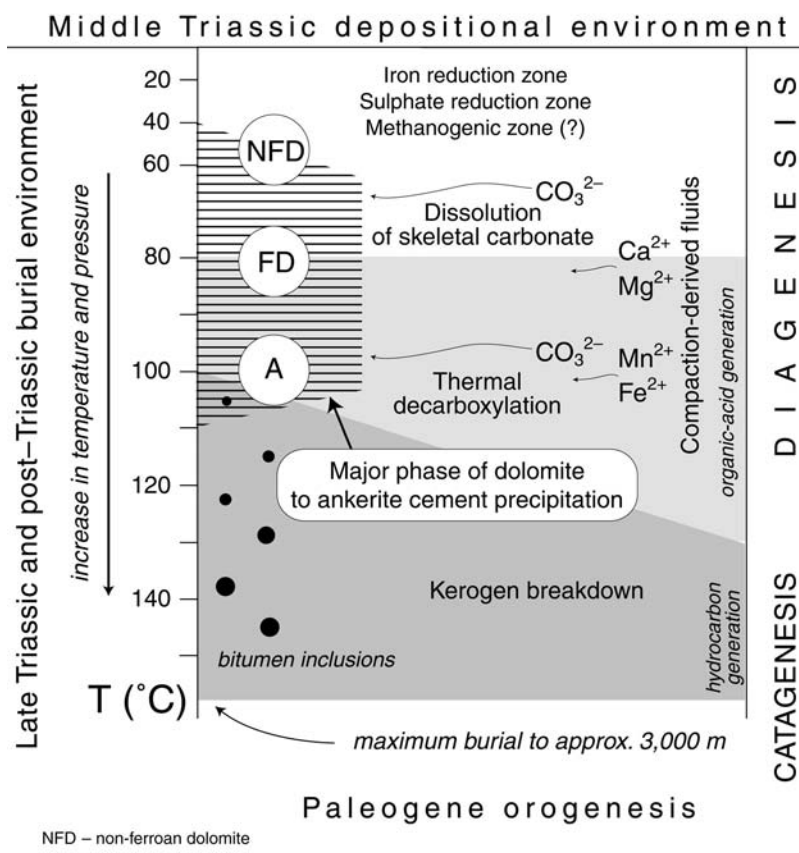


Fig. 11. Location of dolomite-ankerite cement in diagenetic history of the Bravaisberget Fm in western Nathorst Land against burial temperatures, relative availability of metal cations and carbonate in pore fluids, and peak generation of organic acids and hydrocarbons.

a spectrum of diagenetic carbonate cements in clastic marine successions (*e.g.* Hendry 2002; Schmid *et al.* 2004; Machent *et al.* 2007).

**Constraints from  $\delta^{13}\text{C}$ .** — The obtained  $\delta^{13}\text{C}$  values of dolomite-ankerite represent various mixtures of the discerned growth sequence (NFD, FD, A). It is however likely that the compositional trend is towards lighter isotopic composition of carbon from NFD to A. Similar trend has been revealed in carbonate cements in the overlying OC-rich Jurassic shales, and attributed to increasing contribution of organic carbon to carbonate pool during burial of the succession (Krajewski *et al.* 2001, Krajewski 2004). The  $\delta^{13}\text{C}$  values indicate that methanogenic carbonate was of no importance in the cement precipitation. They suggest that inorganic and skeletal carbonate was the dominant carbonate source during first stages of cement precipitation (NFD), which shifted to a mixture of inorganic/organic sources dur-

ing burial (FD, A). Organic acid generation and their thermal decarboxylation seem to have been the primary process of formation of organogenic carbonate, supported by kerogen breakdown at the end of ankerite precipitation. The apparent lack of methanogenic carbonate carbon within the diagenetic carbonate cements seems to be a typical feature of the Mesozoic OC-rich succession in Svalbard, suggesting early kerogenization of organic matter (Krajewski 2004). Most of dolomite and ankerite cements described so far from clastic successions show similar ranges of  $\delta^{13}\text{C}$  values that point to mixed inorganic/organic carbonate sources for cement precipitation (*e.g.* Klein *et al.* 1999; Mansburg *et al.* 2008; Sliaupa *et al.* 2008).

**Constraints from  $\delta^{18}\text{O}$ .** — The oxygen isotope composition of dolomite-ankerite cement can be used to calculate its precipitation temperatures if the composition of precipitating water is known or assumed, and equilibrium relationships controlling  $\delta^{18}\text{O}$  are assumed (Fritz 1976). To our knowledge there are no studies attempting to reconstruct oxygen isotopic composition of the Mesozoic porewaters in the Svalbard sedimentary succession on the basis of analysis of fluid inclusions in diagenetic minerals. However, the analyses presented in this paper suggests that dolomite-ankerite cement in the Bravaisberget Fm developed from intraformational, compaction-derived fluids, which were likely to roughly maintain oxygen isotopic composition of the original marine pore water (Krajewski *et al.* 2001, *for discussion*). Assuming  $\delta^{18}\text{O}$  composition to be in the range from 0‰ to -5‰ VSMOW, the calculated mean temperatures of precipitation fall between 50°C and 100°C, and between 40°C and 90°C, depending on whether dolomite-water or ankerite-water fractionation equation was used (Fig. 10). Because of compositional mixtures of the cement (NFD, FD, A), the real temperature ranges should have been far wider. This is consistent with progressive cement development from early post-sulphidic to early catagenic environments.

## Relation to other ankerite cements in the Mesozoic succession

Ankerite cements were also revealed in OC-rich intervals of the Jurassic (Agardhfjellet Fm) and Cretaceous (Carolinefjellet Fm) succession that overlies the Triassic strata in Svalbard, though NFD cements were not (Krajewski *et al.* 2001; Krajewski 2002, 2004; Krajewski and Luks 2003). Only a minor part of these ankerites shows petrographic, compositional, and isotopic similarities to the ankerite described herein (Figs 5, 9). Most ankerites from the younger formations show oxygen isotopic composition suggesting higher temperatures of precipitation (Fig. 10). These data point to intraformational sources of precipitating fluids for each of the OC-rich intervals rather than to a common origin of the ankerites throughout the succession. Unique for the Triassic strata is compositional trend

from NFD through FD to A. It is observed in OC-rich succession of both the shallow shelf Bravaisberget Fm in western Spitsbergen and the deep shelf Botneheia Fm in central Spitsbergen and eastern Svalbard (Krajewski 2008).

## Conclusions

Petrographic, major element geochemical, and stable carbon and oxygen isotopic analyses of the dolomite-ankerite cement in OC-rich succession of the Bravaisberget Fm suggest its origin over a range of diagenetic and burial environments, from early post-sulphidic to early catagenic (Fig. 11). The compositional trend observed in this cement (NFD, FD, A) reflects evolution of intraformational, compaction-derived marine fluids that was affected by dissolution of biogenic carbonate, clay mineral and iron (hydr)oxide transformations, and thermal decomposition of organic carbon (decarboxylation of organic acids, kerogen breakdown). These processes operated during Late Triassic and post-Triassic burial history over a temperature range from approx. 40°C to more than 100°C, and contributed to the final stage of cementation of the primary pore space of coarser-grained beds and intervals in the OC-rich succession.

**Acknowledgements.** — The fieldwork in Spitsbergen was carried out in summer seasons 2007 and 2008. It was supported by research projects of the Ministry of Science and Higher Education No. N 307 069 32/4103 and IPY/297/2006. We thank Bożena Łącka and Ryszard Orlowski, Institute of Geological Sciences, Polish Academy of Sciences for XRD and EDS analyses, respectively. The carbon and oxygen isotopic analysis was done at the Stable Isotope Laboratory PAS in Warszawa.

## References

- CURTIS C.D. 1987. Inorganic geochemistry and petroleum exploration. In: J. Brooks and D. Welte (eds) *Advances in Petroleum Geochemistry 2*. Academic Press, London: 91–140.
- FISHER R.S. and LAND L.S. 1986. Diagenetic history of the Eocene Wilcox sandstones and associated waters, South-Central Texas. *Geochimica et Cosmochimica Acta* 50: 551–562.
- FRITZ P. 1976. Oxygen and carbon isotopes in ore deposits in sedimentary rocks. In: K.H. Wolf (ed.) *Handbook of Strata-Bound and Statiform Ore Deposits. I. Principles and General Studies 2. Geochemical Studies*: 191–215.
- HARLAND W.B. 1997. The Geology of Svalbard. *Geological Society London Memoir* 17: 521 pp.
- HENDRY J.P. 2002. Geochemical trends and palaeohydrological significance of shallow burial calcite and ankerite cements in Middle Jurassic strata on the East Midlands Shelf (onshore UK). *Sedimentary Geology* 151: 149–176.
- KLEIN J. S., MOZLEY P., CAMPBELL A. and COLE R. 1999. Spatial distribution of carbon and oxygen isotopes in laterally extensive carbonate-cemented layers: implications for mode of growth and subsurface identification. *Journal of Sedimentary Research* 69: 184–191.

- KARCZ P. 2008. *Origin of the Black Shale Facies in the Triassic of Spitsbergen on the Basis of Geochemical Indices*. Unpublished PhD Thesis. Institute of Geological Sciences, Polish Academy of Sciences, Warszawa, Poland, 140 pp. (In Polish)
- KRAJEWSKI K.P. 2000a. Phosphogenic facies and processes in the Triassic of Svalbard. *Studia Geologica Polonica* 116: 7–84.
- KRAJEWSKI K.P. 2000b. Isotopic composition of apatite-bound sulphur in the Triassic phosphogenic facies of Svalbard. *Studia Geologica Polonica* 116: 85–109.
- KRAJEWSKI K.P. 2000c. Diagenetic recrystallization and neoformation of apatite in the Triassic phosphogenic facies of Svalbard. *Studia Geologica Polonica* 116: 111–137.
- KRAJEWSKI K.P. 2000d. Phosphorus concentration and organic carbon preservation in the Blanknuten Member (Botneheia Formation, Middle Triassic) in Sassenfjorden, Spitsbergen. *Studia Geologica Polonica* 116: 139–173.
- KRAJEWSKI K.P. 2000e. Phosphorus and organic carbon reservoirs in the Bravaisberget Formation (Middle Triassic) in Hornsund, Spitsbergen. *Studia Geologica Polonica* 116: 175–209.
- KRAJEWSKI K.P. 2002. Catagenic ankerite replacing biogenic calcite in the Marhøgda Bed (Jurassic), Sassenfjorden, Spitsbergen. *Polish Polar Research* 23: 85–99.
- KRAJEWSKI K.P. 2004. Carbon and oxygen isotopic survey of diagenetic carbonate deposits in the Agardhfjellet Formation (Upper Jurassic), Spitsbergen: preliminary results. *Polish Polar Research* 25: 27–43.
- KRAJEWSKI K.P. 2008. The Botneheia Formation (Middle Triassic) in Edgeøya and Barentsøya, Svalbard: lithostratigraphy, facies, phosphogenesis, paleoenvironment. *Polish Polar Research* 29: 319–364.
- KRAJEWSKI K.P. and LUKS B. 2003. Origin of “cannon-ball” concretions in the Carolinefjellet Formation (Lower Cretaceous), Spitsbergen. *Polish Polar Research* 24: 217–242.
- KRAJEWSKI K.P., KARCZ P., WOŹNY E. and MØRK A. 2007. Type section of the Bravaisberget Formation (Middle Triassic) at Bravaisberget, western Nathorst Land, Spitsbergen, Svalbard. *Polish Polar Research* 28: 79–122.
- KRAJEWSKI K.P., ŁĄCKA B., KUŹNIARSKI M., ORŁOWSKI R. and PREJBISZ A. 2001. Diagenetic origin of carbonate in the Marhøgda Bed (Jurassic) in Spitsbergen, Svalbard. *Polish Polar Research* 22: 89–128.
- LAND L.S. 1985. The origin of massive dolomite. *Journal of Geological Education* 33: 112–125.
- MACHENT P.G., TAYLOR K.G., MACQUAKER J.H. S. and MARSHALL J.D. 2007. Patterns of early post-depositional and burial cementation in distal shallow-marine sandstones: Upper Cretaceous Kenilworth Member, Book Cliffs, Utah, USA. *Sedimentary Geology* 198: 125–145.
- MANSBURG H., MORAD S., SALEM A., Marfil R., EL-GHALI M.A.K., NYSTUEN J.P., CAJA M.A., AMOROSI A., GARCIA D. and LA IGLESIAS A. 2008. Diagenesis and reservoir quality evolution of Paleocene deep-water marine sandstones, the Shetland-Faroes Basin, British continental shelf. *Marine and Petroleum Geology* 25: 514–543.
- MØRK A., KNARUD R. and WORSLEY D. 1982. Depositional and diagenetic environments of the Triassic and Lower Jurassic succession of Svalbard. In: A.F. Embry and H.R. Balkwill (eds) Arctic Geology and Geophysics. *Canadian Society Petroleum Geologists Memoir* 8: 371–398.
- MØRK A., EMBRY A.F. and WEITSCHAT W. 1989. Triassic transgressive-regressive cycles in the Sverdrup Basin, Svalbard, and the Barents Shelf. In: J.D. Collinson (ed.) *Correlation in Hydrocarbon Exploration*. Graham & Trotman, London: 113–130.
- MØRK A., DALLMANN W.K., DYPVIK H., JOHANNESSEN E.P., LARSEN G.B., NAGY J., NØTTVEDT A., OLAUSSEN S., PČELINA T.M. and WORSLEY D. 1999. Mesozoic lithostratigraphy. In: W.K. Dallmann (ed.) *Lithostratigraphic Lexicon of Svalbard. Review and Recommendations for Nomenclature Use. Upper Palaeozoic to Quaternary Bedrock*. Norsk Polarinstitutt, Tromsø: 127–214.

- SCHMID S., WORDEN R.H. and FISHER Q.J. 2004. Diagenesis and reservoir quality of the Sherwood Sandstone (Triassic), Corrib Field, Slyne Basin, west of Ireland. *Marine and Petroleum Geology* 21: 299–315.
- SCOTCHMAN I.C. 1989. Diagenesis of the Kimmeridge Clay Formation, onshore UK. *Journal of Geological Society London* 146: 285–303.
- SLIAUPA S., CYZIENE J., MOLENAAR N. and MUSTEIKYTE D. 2008. Ferroan dolomite cement in Cambrian sandstones: burial history and hydrocarbon generation of the Baltic sedimentary basin. *Acta Geologica Polonica* 58: 27–41.
- WOŹNY E. (in preparation). Diagenesis of pore space in the Bravaisberget Formation (Middle Triassic) in Spitsbergen.

Received 30 October 2008

Accepted 3 August 2009